Relationship of the discontinuities and the rock blasting results

Article *in* Вісник Дніпропетровського університету Геологія географія · March 2018

DOI: 10.15421/111821

CITATIONS
4

READS
1,161

4 authors:

Sami Yahyaoui

13 PUBLICATIONS **8** CITATIONS

SEE PROFILE

Hafsaoui Abdellah

Badji Mokhtar - Annaba University

35 PUBLICATIONS **81** CITATIONS

SEE PROFILE

A. Aissi

Université de M'sila

10 PUBLICATIONS **11** CITATIONS

SEE PROFILE

Aissa Benselhoub

Environmental Research Center CRE-Annaba-Algeria

132 PUBLICATIONS **136** CITATIONS

SEE PROFILE

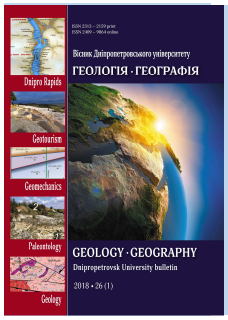

Sami Yahyaoui, Abdellah Hafsaoui,
Adel Aissi, Aissa Benselhoub Dniprop. Univer. bulletin, Geology, geography., 26(1), 208-218.

Relationship of the discontinuities and the rock blasting results

S.Yahyaoui[1], A. Hafsaoui[1], A.Aissi[2], A. Benselhoub[3]

[1]*Badji Mokhtar University, Annaba, Algeria,syahyaoui67@yahoo.fr*
[2]*Ecole Nationale Supérieure des Mines et Métallurgie, Algérie,adeld85@gmail.com*
[3]*State Agrarian and Economic University, Dnipro, Ukraine,benselhoub@yahoo.fr*

Received 12.12.2017
Received in revised form 21.02.2018
Accepted 11.03.2018

Abstract. The Geological discontinuities such as joint are the most common discontinuities present in the rock mass. A model scale study was carried out to evaluate the effect of the joints on rock blasting. Single hole tests at three selected burdens (optimum, less than optimum and more than optimum) were done on six different joint orientations. The joint orientation angles were 0°, 30°, 60°, 90°, 120° and 150° rotating in anticlockwise direction from the floor of the bench in a plane perpendicular to the free face. Bench models of dimensions 515x335x215 mm with a bench height of 50 mm were prepared by binding sandstone slabs of 25 mm thickness with an adhesive. The models were blasted by n°6 electric detonators. The dynamic and static properties of sandstone are given. The bench crater formed and the fragmentation produced were predominantly influenced by the position of charge with respect to the joint orientation. Severe toes were noticed in models with vertical joints and with joints dipping away from the face. Over breaks were observed in horizontally bedded models and in models with joints dipping towards the free face. Over breaks were observed in horizontally bedded models and in models with joints dipping towards the free face. The size of the broken fragments at 20 mm burden was found to be finer than the fragments obtained at 30 mm and 40 mm burdens for all joint orientations except vertical.

Keywords: Fragmentation; model rock blasting; discontinuities; rock mass, bench blasting

Взаємовідношення між тріщинуватістю і результатами підривання порід

С.Яхяуі[1],А.Хафсауі[1],А.Аіссі[2],А.Бенселгуб[3]

[1]*Університет Баджі Мохтар, Аннаба, Алжир*
[2]*Національная школа гірничої промисловості та металургії, Алжир*
[3]*Державний аграрний і економічний університет, Дніпро, Україна*

Анотація. Геологічні розриви, такі як тріщини, є найбільш поширеними порушеннями, присутніми в гірській масі. Було проведено комплексне масштабне дослідження, яке дозволило оцінити вплив тріщинуватості на бризантне здрібнення порід вибухом. Тестування одиночних дірок на трьох вибраних навантаженнях (оптимум, менше, ніж оптимум і більше, ніж оптимум) було виконано на шести різних орієнтаціях суглобів. Спільні кути орієнтації були 0 °, 30 °, 60 °, 90 °, 120 ° та 150 °, обертаючись проти годинникової стрілки від підлоги лави в площині, перпендикулярній вільній поверхні. Ламельні моделі розмірів 515x335x215 мм зі стійкою висотою 50 мм були підготовлені шляхом з'єднання піщаникових плит товщиною 25 мм з клеєм. Моделі були підірвані електричними детонаторами № 6. Дані динамічні та статичні властивості пісковика. Сформований лавровий кратер, і утворену фрагментацію переважно впливає положення заряду щодо орієнтації суглобів. Важкі пальці були помічені в моделях з вертикальними суглобами і зі з'єднаннями, що опускаються від обличчя. Понад перерви спостерігалися в горизонтально сплячих моделях і в моделях з суглобами, що падали до вільного обличчя. Понад перерви спостерігалися в горизонтально сплячих моделях і в моделях з суглобами, що падали до вільного обличчя. Розмір зламаних фрагментів на навантаженні 20 мм виявився більш тонким, ніж фрагменти, отримані при навантаженні 30 мм та 40 мм для всіх орієнтацій спільноти крім вертикальних.

Ключові слова: фрагментація; модельний розкол; розриви; гірська маса, стендові вибухові роботи

Introduction and previous work. It is established that the geological discontinuities present in the rock mass affect the blasting results considerably.This is represent part of the programm of research of the Natural Ressources Engineering. Rock mass properties are important parameters in a blast design; and

understanding the influence of geological discontinues and physic mechanical properties of rock is fundamental to optimum fragmentation. The jointed rocks give poorer fragmentation than unjointed rocks because of the attenuation of stress waves and the escape of gases through joints. The geological discontinuities also create in an imbalance in the distribution of charge and produce uneven fragmentation and breakage (Ash, 1961; Dick, and Olson, 1972; Kim, 2010).

The emergence of cheaper blasting agents (e.g. ANFO) has increased the trend towards larger diameter blast holes with correspondingly larger burdens and spacings. Therefore, the effects of geological discontinuities have become more pronounced because a larger number of discontinuities may be encountered in between in consecutive blast holes. The Investigations by Ash and Hafsaoui& al. (Ash, 1973; Hafsaoui and Talhi, 2009)indicated that the fractures induced by blasting would follow the discontinuity planes and oriented towards free face. He has also found that geological discontinuities cause a rock mass to divide into segments by providing preferred directions for radial and flexural fractures.

Effect of Joints on Blasting Results. Amongst the geological discontinuities, joints are the most common in many rock types. These are defined as planes of weakness within a rock mass along which there has been no visible movement.

There will be difference in the transmission of the stress waves through the Joints depending on whether the Joint is tight, open or filled (Kolsky, 1953; Goldsmith, 1967; Hafsaoui and Talhi, 2011). The tight joints do not affect the transmission of stress waves whereas the open and filled joints introduce an acoustic impedance mismatch and reflect the stress waves. If the reflected wave is sufficiently strong, internal spalling takes place. The radial cracks which the strain wave would have formed in a massive rock are prematurely interrupted by the joint.

Whenever, an open joint intersects the charged section of the blast hole, the gases expand the joint by wedging action and may escape through it without performing the useful work. If the joint extends from the blast hole wall to the face or top of the bench, the premature venting of the gases create air blast and/or fly rock problems in addition to the poor fragmentation and uneven breakage.

In the works (Belland, 1968; Talhi et al., 2003) reported that the fragmentation improved considerably by orienting the free face parallel to and on the dip side of the principal joint planes. In the work (Gnirk and Pfleider, 1968; Larson and Pugleise, 1974) found that the shape of the crater was influenced by the orientation of free face with respect to the planes of weakness. It has been found that the small scale bench blasts, found poor breakage when the row of the blast holes was oblique to the joint direction and better results were obtained when the row of the blast holes was parallel to the joint direction. In the work (Bhandari, 1974) the crater tests found a stepped profile in horizontal sandstone beds. The studies of two extreme cases of joint orientation (viz. horizontal and vertical) and found that average fragment size was affected by joint orientation and burden significantly (Singh et al., 1980). Their results also indicated that the mass of fragments was more influenced by burden than joint orientation.

Cementing Materials. The type of the cementing material in the joint exerts considerable influence on blasting results, because the strength of the rock mass and the degree of attenuation of stress waves depend on the cementing material (Wild, 1977; Bjarnholt and Skalare, 1981). It has been found that the attenuation of stress waves depends on the width of the joint and the impedance of the cementing material (Johnson, 1962).

Model Scale Blasting. It is always better to conduct the blasting experiments on full scale so that they include the structural discontinuities present in the rock mass. This type of work requires handling of large volumes of broken material and thus makes the experiment expensive and difficult. That is why, only a few field studies were undertaken where all the blasted fragments were recovered and screened (Haller et al., 1972; Smith, 1976) have overcome this drawback by conducting the experiments on a reduced scale in in situ rock.

The validity of model scale tests for studying the blasting phenomena has been shown by different authors (Langefors, 1959; Just and Henderson, 1971). The results obtained from the small scale blasting are only qualitative because of the inability to provide the required rock and explosive characteristics to meet similitude requirements (Martin and Murphy, 1963; Da Gama, 1970). However, model blast provides quantitative results amongst themselves.

Site and sample details. A large, intact block of sandstone was obtained from Hadjar soud quarry which is situated 7 kilometers on the outskirts of Azzaba and is an opencast site (see fig.1) (Algeria). Lithologically, the rock is a red, medium grained, hard cemented sandstone. A sample of the rock was desegregated by gentle pressure with a pestle and mortar, taking care not to crush individual grains, and the particle size distribution and the particle specific gravity were determined. It was found that

85 percent of the particle fell in the medium sand range (0.2- 0.6mm) and ten per cent in the fine sand range (0.06-0.2mm) and that the particle specific gravity was 2.66.

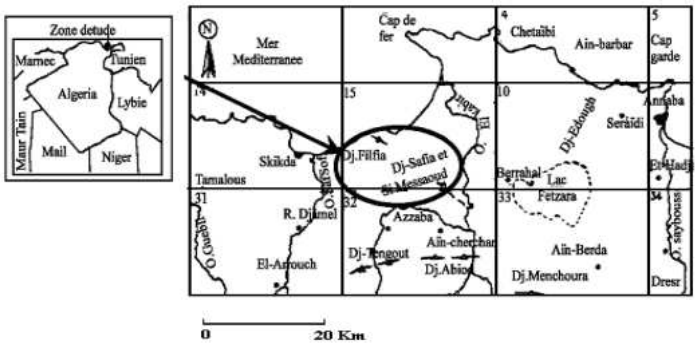

Fig.1. Location map of the study area (Azzaba region)

Properties of sandstone materials. Before blasting the sandstone material properties were determined in a static and dynamic program as follows. The results are summarized in Table 1.

Table1. Summary of the sandstone materials testing

Property	Mean value
Uniaxial compressive strength. C_0 (MPa)	37
Tensile strength, T (MPa)	3.4
Shear strength, ד(MPa)	11
Density, γ (g/cm^3)	2.25
P-wave velocity, C_p (m/s)	4000
S- wave velocity C_s (m/s)	2429
Young's modulus static, E (GPa)	24
Young's modulus dynamic , E_d (GPa)	28
Poisson's Ratio static, μ	0.15
Poisson's Ratio dynamic, μ_d	0.21

The representative cores are obtained from a block, sandstone sample; 38 mm rock cores were cut from it. All core samples were cut to length/diameter of 2.5. The ends of the cores were ground flat and parallel. The diameter and length of each specimen were measured and the mass of each specimen was determined immediately before testing.

The affixing to the specimens of two lateral and two axially oriented foil strain gauge type N22-FA-5-120-H. These pairs are placed diametrically opposite each other and located centrally on the specimen. During testing the pairs are connected up with pairs of gauges on "dummy" sample away from the machine to give temperature variation compensation. This Wheatstone bridge is formed and strain changes are monitored by changes in the voltage across the bridge.

The compression tests were carried out in a fast-response, closed-loop, programmable testing machine. To carry out a test, the specimen was inserted in the testing machine between platens having the same diameter as the specimen. The program was switched on and the specimen was then displaced at a constant rate of 2x10-3 mm seconds, corresponding to an axial strain rate of about 3x10-3 per cent/seconds displacement was thus the independent variable and force was the dependent variable. Failure was then controlled beyond the peak force because the displacement was programmed to increase at a constant rate, regardless of whether this necessitate a rise or fall in applied force. The load was monitored with a pressure transducer and a complete force-displacement curve obtained for each specimen on an X-Y recorder. Remote X-Y chart recorder that was used to monitor the axial and lateral displacement detected by the strain gauges additionally monitored axial load.
The load displacement curves obtained from the X-Y recorder was converted to stress-strain curves by dividing the load by the original cross-sectional area of the specimen to give stress and by dividing the displacement by the original length of the specimen to give strain.

The uniaxial compressive strength (Co) was obtained from the peak of each curve. Young's modulus (E) and Poisson's ratio (μ) were obtained from the stress-strain axial and lateral curves. The details are given in Talhi et al. The method used to

determine the tensile strength (T) of the sandstone was the indirect tensile strength. The Brazilian test was performed using 38 mm diameter specimen and thickness equal to the specimen radius. From the load at failure and the specimen dimensions, the tensile strength was calculated. The shear box was used to determine the shear strength (τ). The specimen and plaster were placed into the shear box and constant holding load was applied by means of a hand operated hydraulic pump. Another such pump was used to apply a shearing load along the shear plane; this load was progressively increased until rupture occurred. Knowing the force applied along shearing plane and the cross sectional area, the shear strength was computed.

The dynamic properties of the sandstone were determined indirectly by measuring the propagation velocities in the sandstone.

In pulse techniques, a mechanical impulse is imported to a specimen. The time required for the transient pulse to traverse the specimen length is used to calculate the wave velocity. The instrumentation consists of a pulse generator, sample holder assembly, a timer stabilizer, an amplifier and an oscilloscope. Two sample holder assemblies were employed. One was used to determine the P-wave velocity (CP) and the other was used to determine the S-wave velocity (CS). The sample holder assembly contains two rectangular (in CP experiments) or triangular (in CS experiments) Pyrex glass plates upon which were placed transducers. The pulse coming directly from the pulse generator was transmitted through the specimen by one glass wedge (driver) and picked by the other (pickup) connected to the amplifier. The amplified signal was fed to an oscilloscope. The wave travel in a specimen was recorded from the timer and checked by the time indicated on the oscilloscope. Knowing CP and CS, dynamic E-modulus (Ed) and dynamic Poisson ration (μd) were calculated.

Experimental method. The model scale blasting can be conducted on various types of rocks and materials depending upon their availability, strength, homogeneity and the type of explosive being used.

In our case, six different joint orientations were chosen for the investigation. They were 0°, 30°, 60°, 90°, 120° and 150° rotating in anticlockwise direction from the floor in a plane perpendicular to the free face (see table 2). The size of each block was 515 x 335 x 215 mm with a bench height of 50 mm (see fig. 2) sandstone slabs of 25 mm thickness were cut to the appropriate size and bound together by an adhesive to prepare the bench models. The adhesive was applied over the whole surface of the slabs to have a uniformly filled joint.

Table 2. Summary of the test series

Angle, degrees (θ)	0			30			60			90			120			150		
Burden, (B)	20	30	40	20	30	40	20	30	40	20	30	40	20	30	40	20	30	40

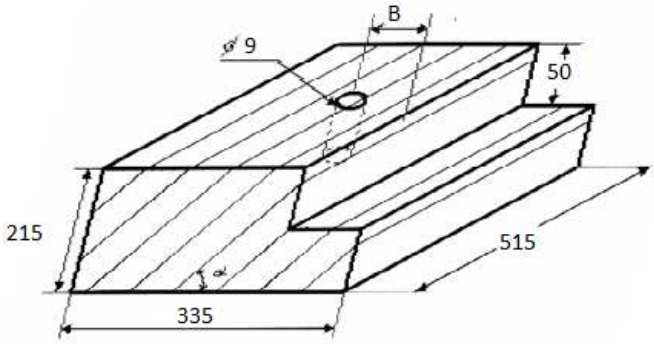

Fig.2. Model configurations used in the blast tests

Optimum fragmentation burden (burden for which "mass-surface was maximized) for unjointed models was found to be 30 mm (Saran, 1981). The burdens (B) chosen for the present investigation were more than an optimum burden (i.e. 40 mm), equal to optimum (i.e. 30 mm) and less than optimum burden (i.e. 20 mm).

A vertical hole of *9*mm diameter was drilled in the center of each block at the selected burden without sub drilling. Each model blasted by a number 6electric detonator and is shown in figure 2.

The broken fragments collected after blasting were subjected to sieve analysis. The sizes of the sieves used were 101.6 mm, 50.8mm, 25.4 mm, 12.7 mm, 5.1 mm, 1.7 mm and 0.5 mm.

Mass surface area and average fragment size were determined for each test. The mass was obtained by weighing the broken fragments collected after each blast. The new surface area of the irregular blasted

fragments was calculated (Heywoud and Pryros, 1998). The mass surface area was obtained by multiplying the mass and new surface area. Average fragment size (AFS) for each test was obtained by the following formula (Pryors, 1965).

$$AFS = \frac{\sum_{i=1}^{7} m_i n_i}{\sum_{i=1}^{7} m_i} \quad (1)$$

Where, m_i =mass of fragments retained in between i^{th} and $(i-1)^{th}$ sieve; and n_i = mean aperture size of i^{th} and $(i-1)^{th}$ sieve.

This, however, gives weightage for larger fragments as this value can be determined even by the material collected on top two sieves.

Al though the term fragmentation has been used in blasting terminology, it has not yet been well defined quantitatively.

The passing size of 80% as a measure of fragmentation in blasting was used (Bond and Whitney, 1959). An attempted to derive fragmentation law for rock blasting was used (Henderson, 1971). The related size distribution for blast design parameters was used (Just, 1973). The authors (Dick, et al., 1973; Denoual and Hild, 2002) studied fragmentation on a reduced scale quantitatively. They related the cumulative mass percentage and sieve size by a simple power curve,

$$y = ax^b \quad (2)$$

Where, y- cumulative weight percentage;
a =y-intercept;
x=sieve size and
b=slope of the curve.

It has also been found that the above curve fits well in fragmentation studies of blasting (Singh et al., 1980). The values of the sieve sizes and cumulative mass percentages obtained in the present investigation gave a straight line equation " y = a + bx ". The correlation coefficient obtained was about 0.92 for all tests.

The coarse fragmentation index' was obtained by dividing the mass percentage of +25.4 mm fragments by the mass percentage of - 25.4 mm fragments. Similarly, the fine fragmentation index got by dividing the mass percentage of -1.7 mm material by mass percentage of +1.7 mm material (Smith, 1976).

The fracture characteristics such as shape of the bench crater, over break, back breaks, toe and overhangs were studied in each model blast. The coarse fragments collected after the blasting was reassembled and an attempt was made to explain the mechanism of failure.

Discussion of results. The discussion of the results is given as follows. The explanation of the fracture characteristics such as over break, back breaks, overhangs, toes etc. in each model after blast.

Joint orientation Θ=0° and B =20 mm**:** The whole burden perpendicular to the blast hole axis was thrown out and a bench crater with 150° angle of the break was formed. The broken fragments and six radial cracks were found around the blast- hole, and for which two extended behind the new face as back breaks. A circumferential crack was observed behind the new face.

It appears that the circumferential cracks were developed due to the radial tensile strains developed by the differential radial movements between the slabs. The 2nd slab containing the explosive charge might have moved more than the 1st and 3rd slabs, which were fixed by an adhesive with the 2nd slab.

Joint orientation Θ=0° and B =30 mm: It was formed in this model a semi-circular shape of the bench crater with large over break. Even though, the radial cracks and the circumferential crack observed in this blast were similar to that noticed in the model with 20 mm burden; the fractured rock behind the face was lifted, creating a large over break.

Joint orientation Θ=0° and B =40 mm**:** It was observed in this model radial cracks and circumferential crack similar to those in the other horizontally bedded models. The fragments were encompassed by the circumferential crack in the 2nd slab was left intact and a stepped bench crater was formed.

Joint orientation Θ=30° and B =20 mm**:** It was created in this model an angle of break about 150°. Due to spalling a thin flaky fragment were obtained.

Joint orientation Θ=30° and B =30 mm**:** In this blast has got severe toe and back breaks. The upward pressure exerted by the expansion of the gases might have developed the back breaks whereas the wedging action of the gases created a cavity nears the II joint. The flaky fragments obtained from the 2nd slab reveal the spalling effect.

Joint orientation Θ=30° and B =40 mm: In this modelthe fracture pattern and the bench crater observed were similar to in the model with 30mm burden, but with a more severe toe and overhangs.

Joint orientation Θ=60° and B =20 mm**:** In this model a bench crater with the 155° angle of the break was formed. Five symmetrically located radial cracks extended beyond the new face as back break. The degree of fragmentation in the 2nd slab was

found to be more than the 3rd slab because of the full explosive charge placed in the 2nd slab.

Joint orientation Θ=60° and B =30 mm**:** It was observed in this model the shape of the bench crater is similar to in the model with 20 mm burden, but with severe toe and less back breaks.

Joint orientation Θ=60° and B =40 mm: In this model the bench crater formed was similar to that observed in the model with 30 mm burden.

Joint orientation Θ=90° and B =20 mm: In this model a wide crater with little toe was created. The fracture pattern noticed after the rearrangement of the broken fragments revealed the combined action of bending, spalling and radial fracturing. As the charge was placed in the II joint, the gases tried to separate the II joint and thus developed a cavity.

Joint orientation Θ=90° and B =30 mm: In this model the bench crater was not uniform and had a severe toe. The fracture pattern observed after reassembling the broken fragments indicated the cantilever bending action in the 2nd slab.

Joint orientation Θ=90° and B =40 mm: The crater observed at 40 mm burden was similar to that developed at 30 mm burden. The fractures noticed after rearranging the broken fragments demonstrate the bending action in the 2nd slab. The back breaks were severe probably due to the less loss of energy.

Joint orientation Θ=120° and B =20 mm: The width and the crater breakage angle in the face was less than those behind the blast hole. The fractured fragments at the bottom of the 3rd slab remained in position as toe.

That is why the coarse fragments were observed from the 2nd slab. The toe and the overhangs were probably due to the resistance offered by the 2nd slab.

Joint orientation Θ=120° and B =30 mm: This blast was similar to that noticed in the model with 20 mm burden, but the burden portion of the 3rd slab remained as toe. The 3rd slab remained as toe because of the resistance offered by the 2nd slab and severe loss of energy. A depression on the unmoved portion of the 3rd slab (i.e. left as toe) depicts the internal spalling effect due to the reflection of stress wave by I joint.

Joint orientation Θ=120° and B =40 mm: This model was similar to that observed in the model with 30 mm burden. The over break in this model extended even in the 4th slab due to charge contained in it.

Joint orientation Θ=150° and B =20 mm: Severe overhangs and little over break was formed in this blast. The 2nd slab was coarsely fractured because of the absorption of stress waves by I and III joints.

Joint orientation Θ=150° and B =30 mm: A new inclined face was developed in this blast. The fractures observed after the rearrangement of the broken fragments indicated the bending action in the 2nd slab.

Joint orientation Θ=150° and B =40 mm: over break formed in this model was less than that observed in the model with 30 mm burden. The fracture study after reassembling the fragments showed that the burden might have fractured by bending.

Fragmentation studies. ***Mass of fragments.*** The mass of fragments collected at burden B= 20 mm was lower than that obtained at burden B= 30 mm except in the vertically jointed models. Mass of fragments increased with a burden in models with joint orientations Θ= 0°, 60° and 120°. In the models with joint orientation Θ=0° and 150°, maximum mass was obtained at the burden B=30 mm. In vertically jointed models, mass of fragments obtained at burdens B = 20 and 40 mm was almost equal and more than that obtained at burden B=30 mm, figure 3.

Mass surface area. The mass surface area did not follow any definite trend with either burden or joint orientation, figure 4.

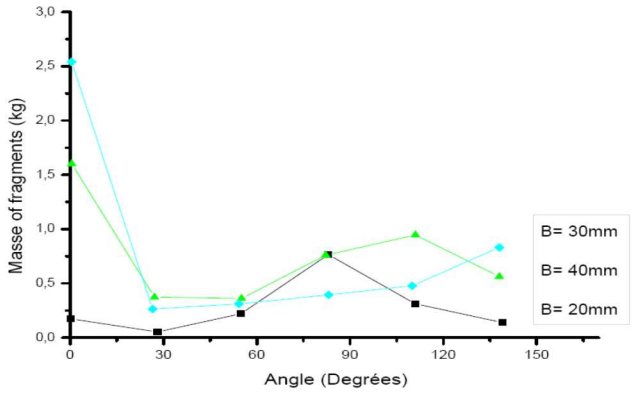

Fig.3. Mass of fragments vs joint orientation

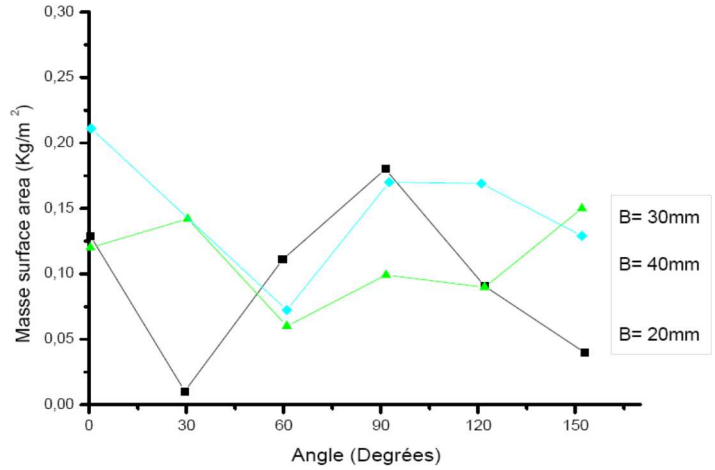

Fig.4. Mass surface area vs joint orientation

Average fragment size.Except with the vertically jointed models (Θ = 90°), average fragment size obtained at 20 mm burden was smaller than the average fragment sizes collected at 30 and 40 mm burdens. The average fragment size increased with increase in burdens in the models with a joint orientation Θ= 30°, 60° and 120°. In the models having joint orientation Θ =0° and 150°, maximum, average fragment size was found at 30 mm burden. In vertically jointed models (Θ = 90°), maximum, average fragment size was obtained at 40 mm burden and minimum at 30 mm burden, figure 5.

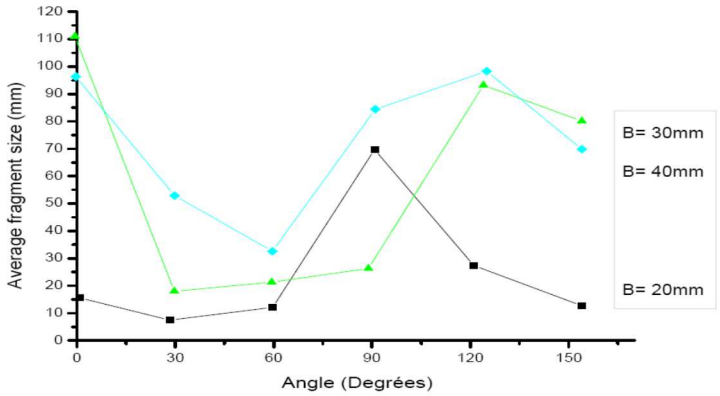

Fig.5. Average fragment size vs joint orientation

Least squares curves.A straight line equation $y = a + bx$ was found to be satisfying the values of cumulative mass percentage and their corresponding sieve sizes for a, l the tests, figure 6. Thus least square lines explain the size distribution of broken fragments collected after blasting. Flatter the lines (lesser the slope), coarser are the fragments.

In horizontally bedded models the least square lines indicated that the fragments collected at 30 mm and 40 mm burdens are more or less similar but coarser compared to the fragments collected at 20 mm burden, figure 6a.

The least squares fit flattened with the increasing burden in the models with a joint orientation Θ= 30°. This indicates the increase of coarse fragments with burden, figure 6b.

The straight lines obtained in the models with joint orientation Θ=60° are very close to each other. This shows that the size distribution of broken fragments collected at all the three burdens is similar to each other, figure 6c.

In vertically jointed models the size distribution of the broken fragments at 20 and 40 burdens were almost akin but coarser compared to the fragments obtained at 30 mm burden, figure 6d.

In the models with a joint orientation Θ = 120°, the size distribution of the fragments became coarser with increasing burden. However, the close and parallel lines obtained at 50 and 40 mm burdens indicate more or less similar size distribution, figure 6e.

The least square lines obtained in the models with joint orientation Θ= 150° show that the size distribution of the broken fragments collected at 30 and 40 mm burdens is similar to each other but coarser compared to the fragments collected at 20 mm burden, figure 6f.

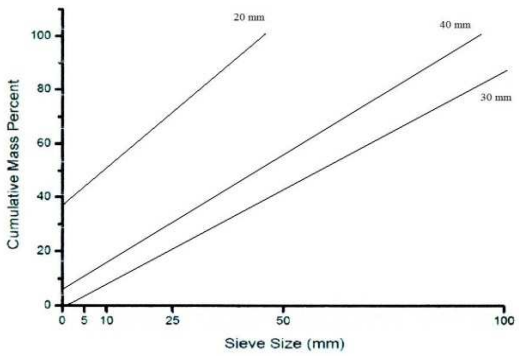

Fig 6a. least square curves Θ=0

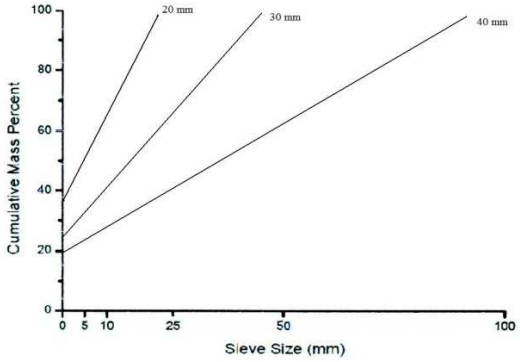

Fig.6b.least square curves Θ=30°

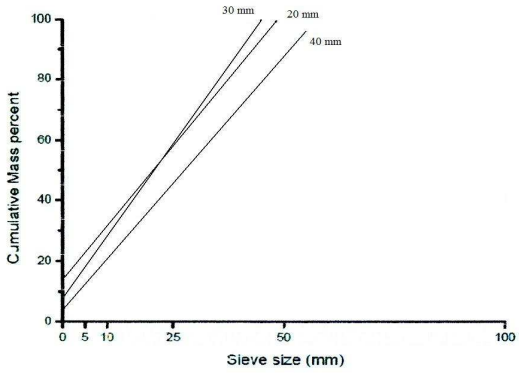

Fig.6c.least square curves Θ=60°

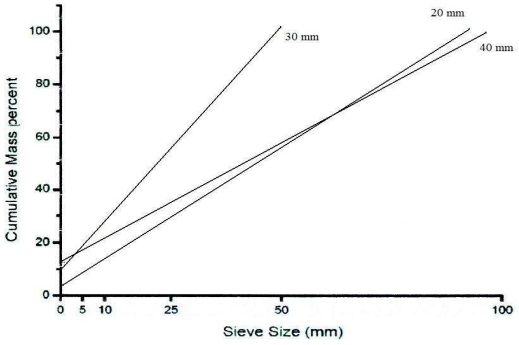

Fig.6d. least square curves Θ=90°

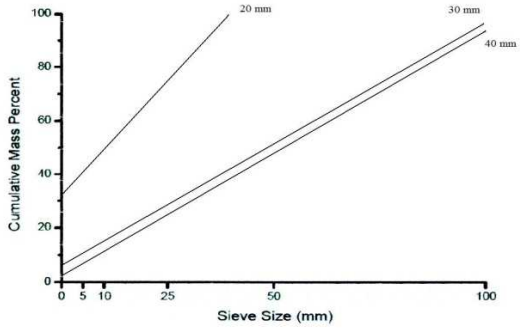

Fig.6e. least square curves Θ=120°

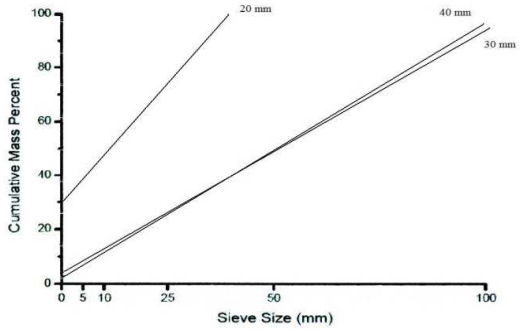

Fig.6f. least square curves Θ=150°

Analysis of the variance of the test results showed that the mass of fragments, mass surface area and slope of least square lines were not affected by burden or Joint orientation significantly. However, the results indicated that the average fragment size was affected by burden significantly at the 5 % level.

Coarse fragmentation index. Except the models with Joint orientations Θ=60° and 90°, coarse fragmentation indices calculated at 20 mm burden were less than 0.5 (very small). The coarse fragmentation index for a particular burden was minimized when the Joints are dipping away from the face at an angle 30° from the floor (Θ= 30°), figure 7.

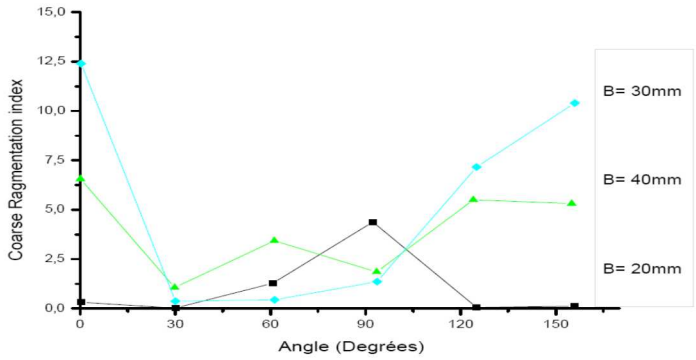

Fig.7. Coarse fragmentation index vs joint orientation

Fine fragmentation index. Except vertically jointed models, fine fragmentation indices found at 20 mm burden were higher than the fine fragmentation indices registered at 30 and 40 mm burdens. For a particular burden, fine 47fragmentation index obtained in the models with Joint orientation Θ=30° was higher compared to other orientations, figure 8.

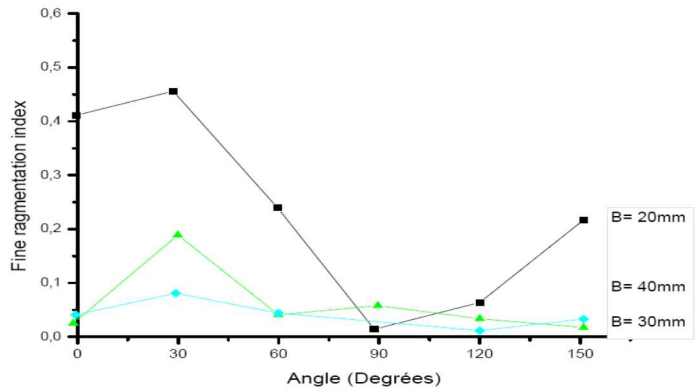

Fig.8. Fine fragmentation index vs joint orientation

The shape of the broken fragments. The coarse fragments collected in horizontally and vertically jointed models were plate shaped with a thickness equal to the slab thickness (i.e. 25 mm). The shape of the large fragments in the models with Joints dipping away from the face (i.e. Θ = 30° and 60°) was oblong, whereas in the models with joints dipping towards the face (Θ = 120° and 150°) it was tabled, figure 9.

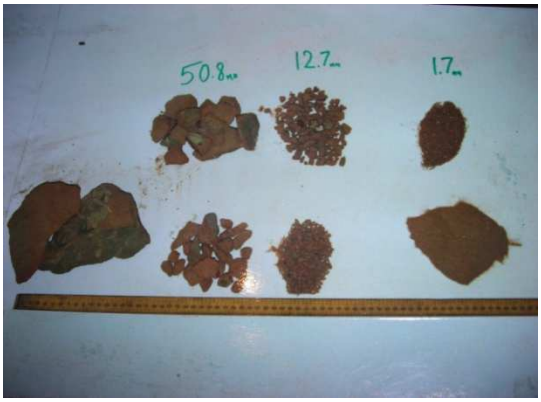

Fig.9. Shape and size of fragments

Conclusions. The following conclusions which can be drawn are as follows:

It appears that the shape and size of the bench crater and the fracture pattern developed were controlled by the position of charge with respect to the Joint orientation. The degree of fragmentation at a particular point in the model was found to depend on the distance of the point from the charge and the number of joints in between the point and the charge.

Spalling at the free face was not observed in the models having joint planes in between the charge and the face. Internal spalling, crushing and cavities were observed near the joint plane in some of the models.

The problem was found to be increasing with a burden in vertical jointed models and in models with joints dipping away from the face. However, toe problem was also observed in some models with joints dipping towards the face. Severe over break was observed in horizontally bedded models and in models with joints dipping towards the face. Except with the vertically jointed models, the mass of fragments and the average fragment size obtained at 20 mm burden was minimized. For a particular burden, the coarse fragmentation index was minimized and the fine fragmentation index was maximized when the joints were dipping away from the face at an angle of 30° from the floor. The size of the broken fragments at 20 mm burden was found to be finer than at 30 and 40 mm burdens for all orientations except vertical. Mass of fragments, mass surface area and slope of least square lines were not affected by burden or joint orientation significantly. However the average fragment size was affected by the burden. The large fragments obtained in horizontally and vertically jointed models were plate shaped with a thickness equal to the slab thickness. The shape was oblong when the joints were dipping away from the face and tabular when the joints were dipping towards the face.

Acknowledgements. The authors are gratefully acknowledged to the Laboratory of Natural Resources and Planning, Badji Mokhtar University, Annaba, Algeria, National Office of Expolsives and all colleagues contributed to conduct this research paper.

References

Ash, R.L. 1961. Drill Pattern and Initiation-Timing Relationships of Multiple Hole Blasting, Quarterly, Colorado School of Mines, Vol. 56, 1, 309-324.

Dick, R.A., Olson, J.J. 1972. Choosing of proper Borehole Size for Bench Blasting, *Mining Engineering,* Vol. 24, 3, 40-46.

Kim, S. J. 2010. An Experimental Investigation of the Effect of Blasting on the Impact Breakage of Rocks. Kingston, Ontario, Canada: The Robert M. Buchan Department of Mining, Queen's University, (Master Thesis).

Ash, R.L. 1973. The Influence of Geological Discontinuities on Rock Blasting, Ph.D. Thesis, University of Missouri Rolla. 87 pp., 2.

Hafsaoui, A., Talhi, K. 2009. Influence of joint direction and position of explosive charge on fragmentation. *Arabian Journal for Science and Engineering,* Vol. 34, 2A., 125-132.

Kolsky, H. 1953. Stress Waves in Solids, Dover Publications, Inc. New York. 10014, Science Education. Volume 52, Issue 5, Inc. 213 p.

Goldsmith, V.. Pulse Propagation in Rocks, *Proceedings, 8th Symposium on Rock Mechanics, New York*, pp. 523-537.(1967)

Hafsaoui, A., Talhi, K. 2011. Instrumented Model Rock Blasting.*Journal of Testing and Evaluation.*Vol. 39, Issue 5, 181-187.

Belland, J.M. 1968. Structure as a Control in Rock Fragmentation Coal Lake Iron Ore Deposited, *The Canadian Mining and Metallurgical Bulletin,* Vol. 59, 647, 323-328.

Talhi, K., Bensaker, B. 2003. Design of a model blasting system to measure peak p-wave stress, *Soil Dynamics and Earthquake Engineering,* Vol. 23, Issue 6, 513-519.

Gnirk, P.F., Pfleider, E.D. 1968. On the Correlation Between Explosive Crater Formation and Rock Properties, *Proceedings, 9th Symposium on Rock Mechanics, Colorado School of Mines,* 321-345.

Larson, W.C., Pugleise, J.M. 1974. Effects of Jointing and bedding Separation on Limestone Breakage at Reduced Scale, R.I 7863, U.S. Bureau of Mines. 1-13.

Bhandari, S. 1974. Blasting in Non-Homogeneous Rocks, *Australian Mining,* Vol. 66, 5, 43-48.

Singh, D.P., Saluja, S.S., Rao, Y.V.A. 1980. A Laboratory Study of Effects of Joints on Rock Fragmentation, *Proceedings, 21st **U.S.** Rock Mechanics Symposium, University of Missouri Rolls.*

Wild, H.W. 1977. Geology and Blasting in Open pits, *Mining Magazine*, March, 1-227.

Bjarnholt, G., Skalare, H. 1981. Instrumented Rock Blasting – Initial experiments in Concrete blocks, SveDeFo Stockholm, report DS 1981 : 16, (in Swedish).

Johnson, J.B. 1962. Small-scale blasting in mortar**.** U.S. Dept. of the Interior, Bureau of Mines. 1-22.

Haller, H.F., Pattison, H.C., Shimizu, B. 1972. Inter-Relationship of In-situ Rock Properties, A.R.P.A. Order 1579, California.

Smith, N.S. 1976. Burden-Rock Stiffness and Its Effect on Fragmentation in Bench Blasting, Ph.D. Thesis, University of Missouri Rolla.

Langefors, V. 1959. Calculations of Charge and Scale Model Trials, *Quarterly, Colorado School of Mines*, Vol. 54, 3, 219-249.

Just, G.D., Henderson, D.S. 1971. Model Studies of Fragmentation by Explosives, *Proceedings, 1st Australian and Newzeland Conference on Geomechanics, Melbrone,* Vol.1, 238-245.

Martin, C.W., Murphy, G. 1963. Prediction of Fracture Due to explosives**,** Engn. Mech. Div. A.S.C.E., Vol. 89, 133-150.

Da Gama, C.D. 1970. Laboratory Studies of Comminution in Rock Blasting, M.S. Thesis, University of Minnesota.

Saran, S. 1981. A Study of Spacing-Burden Ratio on Rock Fragmentation by Blasting, B.Tech. Project, Banaras Hindu University.

Heywoud, H., Pryros, E., J. Applied of sizing analysis to mill practice, Trans. I.M.M., Vol. 55, pp. 405-425.

Pryors, E.J. 1965. Mineral Processing, Elsvica Publishing Co. Ltd., London, 150-151.

Bond, F.C., and Whitney, B.B. 1959. The Work Index in Blasting, Quarterly Colorado School of Mines, Vol. 54, 77-82.

Henderson, D.S. 1971. Model Studies of Fragmentation by Concentrated and Linear Explosive. Charges, M. Eng. Sc. Thesis, University of Queesland..

Just, G.D. 1973, The Application of size Equations to Rock Breakage by Explosives, *Proceedings, National Symposium on Rock Fragmentation, Adlaide,* 18-23.

Dick, R.A., Fletcher, L.R., D'Andrea, D.V. 1973. A Study of Fragmentation from Bench Blasting in Limestone at a Reduced Scale, R.I. 7704, U.S. Bureau of Mines.

Denoual, C., Hild., F. 2002. Dynamic Fragmentation of Brittle Solids: a Multi-Scale Model. *Eur. J. Mech.A/Solids,*vol. 21, 1, 105–120.